EFFECTS OF COLLAGEN MICROSTRUCTURE ON THE MECHANICS OF THE LEFT VENTRICLE

J. OHAYON AND R. S. CHADWICK
Theoretical Biomechanics Group, Biomedical Engineering and Instrumentation Branch, Division of Research Services, National Institutes of Health, Bethesda, Maryland 20892

ABSTRACT The microstructure of the collagen sheath or weave surrounding a myocyte and the collagen struts interconnecting neighboring myocytes is incorporated into a fluid–fiber–collagen continuum description of the myocardium. The sheaths contribute to anisotropic elasticity, whereas the struts contribute to an isotropic component. Elastic moduli of the composite myocyte–sheath complex and the strut matrix are estimated from existing passive biaxial loading data from sheets of canine myocardium. The contribution of the sheath to the elasticity of the myocyte–sheath complex is critically dependent on the helical pitch angle. Calculations for a cylindrical model of the left ventricle using both a fluid–fiber and fluid–fiber–collagen stress tensor show that the collagen strut matrix tends to limit muscle fiber lengthening; increase myocardial tissue pressure during systole, with endocardial tissue pressure exceeding left ventricular pressure; decrease tissue pressure during diastole, and thus facilitate myocardial blood flow; and aid filling during ventricular relaxation by providing a suction effect that relies on a release of stored elastic energy from the previous contraction. Calculations show that this energy is stored mostly in the collagen struts.

INTRODUCTION

A sound theoretical formulation for the elastic properties of the myocardium is fundamental to the description of left ventricular (LV)[1] mechanics. A recent approach to a mathematical description of the heart considered the cardiac muscle as a fluid–fiber continuum, and neglected the presence of collagen (Peskin, 1975; Feit, 1979; Chadwick, 1981, 1982, Tözeren, 1983; Pelle et al., 1984; Ohayon et al., 1987; and Ohayon and Chadwick, 1987). However, recent measurements on myocardial sheets (Demer and Yin, 1983) imply that the passive myocardium is not as anisotropic as the fluid–fiber continuum suggests (Fung, 1984). In this work, we utilize a fluid–fiber–collagen continuum stress tensor to infer the passive elastic moduli from experiments, and interpret the results in terms of the myocardial microstructure.

Robinson et al. (1986) have presented strong arguments that collagen plays an important role in the mechanism of LV filling by storing energy from the previous contraction to provide a suction effect during relaxation. We investigate this hypothesis by computing the minimum cavity pressure when filling is prevented and the systolic strain energy of the different constituents of the connective tissue.

BACKGROUND, THEORY, ANALYSIS, AND RESULTS

Collagen Structure in the Myocardium

Anatomical observations have shown that cardiac muscle tissue has a highly specialized architecture. This structure is composed primarily of cardiac muscle cells, or myocytes, arranged in a more or less parallel weave that we idealize as "muscle fibers." We shall denote the local direction of this group of cells by the unit vector $\vec{\tau}$. Streeter's (1979) measurements have shown that the fiber direction field defines paths on a nested family or toroidal surfaces of revolution in the wall of the heart. His results show a continuously changing orientation $\vec{\tau}$ of the muscle fibers through the wall, circumferential near the midwall and progressively more inclined with respect to the equatorial plane when moving toward either the epicardium or the endocardium.

Other studies (Borg and Caulfield, 1979, 1981; Caulfield and Borg, 1979; Borg et al., 1981; Robinson et al., 1983, 1986, and 1987) on the connective tissue of mammalian heart muscle give a detailed description of the extracellular structures and their arrangement relative to cardiac muscle cells (Fig. 1). Each muscle fiber is surrounded by a sheath of connective tissue (epimisium). This sheath contains a large number of collagen fibers and far fewer elastin fibers. Observations on papillary muscle show a regular geometrical arrangement of this sheath in the form of a crisscross weave. Such a network could protect the sarcomere from overstretching. When the fiber is stretched to sarcomere lengths between 2.3 and 2.5 μm, the collagen fibers are essentially aligned along the axis and the muscle fiber, thus providing a structure more resistant to deformation (Robinson et al., 1983).

The connective tissue is also composed of struts formed by bundles of collagen fibrils (endomisium) that interconnect adjacent muscle fibers. These struts have a diameter ranging between 120 and 150 nm (Caulfield and Borg, 1979). They appear to be quite slack in the stress-free state

1. *Abbreviation used in this paper:* LV, left ventricular.

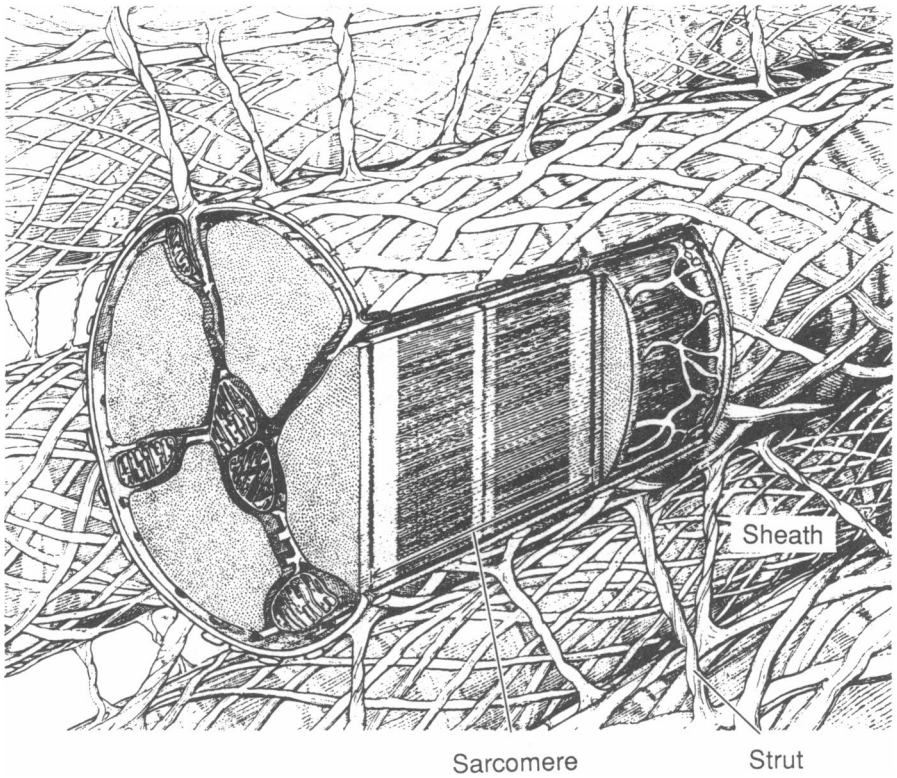

FIGURE 1 Schematic view of the microstructure of the collagen sheath surrounding myocytes and the collagen struts interconnecting neighboring myocytes. *From* The heart as a suction pump. T. F. Robinson, S. M. Factor, and E. H. Sonnenblick. Copyright © April 1986 by Scientific American, Inc. All rights reserved.

and are aligned primarily transverse to the muscle fiber direction, but branch in quite random directions before attachment to adjacent myoctes. This hierarchy of branching structures leads, we believe, to an essentially isotropic component to the heart structure. The volume occupied by collagen in the left ventricle was measured and expressed as a percentage of total cross-sectional area occupied by tissue. The values obtained by Lenkiewicz et al. (1972) show that the proportion of projected area of myocardium occupied by collagen is ~30%.

To be consistent with our description of the components of the myocardium we specify some definitions and subscript notation that are used in this study: (*a*) The collagen strut matrix is the endomisium; subscript "cm." (*b*) The collagen sheath is the epimisium; subscript "cs." (*c*) The muscle fiber is a group of myocardial cells without the epimisium; subscript "mf." (*d*) The composite fiber is the muscle fiber with epimisium (myocyte–sheath complex); subscript "f." (*e*) A collagen fiber from the sheath has the subscript "cf."

Continuum Stress Tensor for the Myocardium

High fluid content acting together with oriented muscle fibers led Peskin (1975) to suggest a continuum fluid–fiber stress tensor to describe the rheology of the heart wall:

$$\sigma_{ij} = -P_h \delta_{ij} + T_f \tau_i \tau_j, \tag{1}$$

where T_f is the tension (force per unit of myocardial area) in the composite fiber, P_h is the hydrostatic fluid pressure in the heart wall, δ_{ij} is the Kronecker symbol, and τ_i is the component of the unit vector in the direction of the composite fiber.

Eq. 1 neglects the isotropic term because of the presence of the collagen struts. To include this additional effect, consider the equilibrium of an elemental tetrahedron, composed of three orthogonal faces and a slanted face with unit normal, $\vec{n}$. The element is oriented in such a way that the local fiber direction is normal to the face in the x, y plane. This element is assumed to be a continuum of fluid, muscle fibers, and collagen. Also, because the element is infinitesimal the variation of the stresses acting on a side can be neglected. The state of stress acting on the tetrahedron is shown in Fig. 2. The different stresses acting on this elementary volume are the pressure P_h due to the fluid, the tension T_f due to the action of the composite fibers, as well as shear and normal stresses S_{ij} due to the isotropic matrix of collagen struts. The stress vector $\vec{\sigma}_n$ acting on the slanted face can be found by requiring the element to be in mechanical equilibrium, with the result:

$$\vec{\sigma}_n = -P_h \vec{n} + T_f(\vec{\tau} \cdot \vec{n})\vec{\tau} + \underset{\sim}{S} \cdot \vec{n}. \tag{2}$$

A stress tensor $\underset{\sim}{\sigma}$ exists having the property $\vec{\sigma}_n = \underset{\sim}{\sigma} \cdot \vec{n}$, where $\underset{\sim}{\sigma}$ is independent of $\vec{n}$. The component form is:

$$\sigma_{ij} = -P_h \delta_{ij} + T_f \tau_i \tau_j + S_{ij}. \tag{3}$$

From classical elasticity theory, S_{ij} is given by:

$$S_{ij} = 2 \mu_{cm} \epsilon_{ij} + \lambda_{cm} e \delta_{ij}, \tag{4}$$

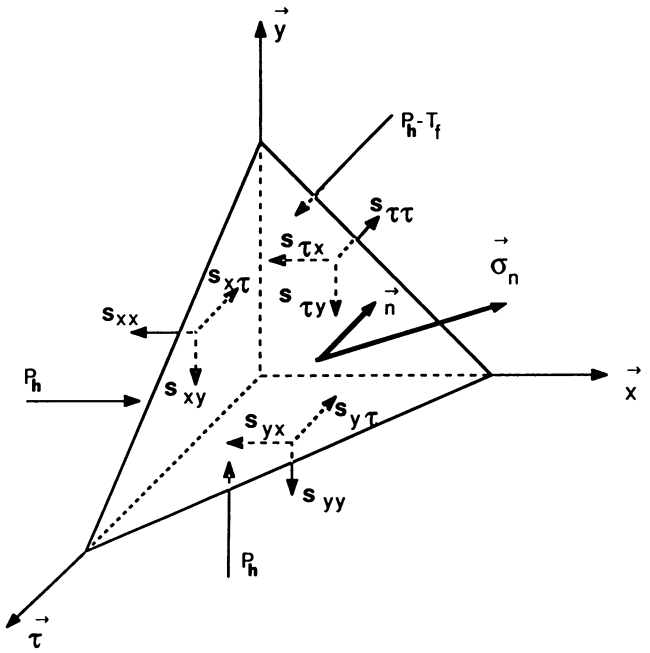

FIGURE 2 Stress components acting on faces of elemental tetrahedral volume of myocardial continuum.

where μ_{cm} and λ_{cm} are the shear modulus and the Lamé's coefficient of the collagen strut matrix, ϵ_{ij} are the components of the Lagrangian strain tensor, and e is the divergence of the displacement field (relative volume expansion). We assume that both the fluid phase and the collagen strut matrix phase are each incompressible. In that case $\lambda_{cm} \rightarrow \infty$ and $e \rightarrow 0$ in such a way that a finite product $\lambda_{cm}e$ exists and can be absorbed into the hydrostatic pressure (Spencer, 1972). Substituting Eq. 4 into Eq. 3 yields:

$$\sigma_{ij} = -P\,\delta_{ij} + T_f \tau_i \tau_j + 2\,\mu_{cm}\,\epsilon_{ij}. \tag{5}$$

In this last expression P now represents the myocardial tissue pressure defined here as the hydrostatic pressure modified by the presence of the collagen strut matrix, i.e.:

$$P = P_h - \lim_{\substack{\lambda_{cm} \rightarrow \infty \\ e \rightarrow 0}} (\lambda_{cm} e). \tag{6}$$

Further elaboration of the concept of myocardial tissue pressure is given in the Discussion.

In the myocardium the muscle fibers themselves contain intracellular fluid. In this formulation no distinction is made between intracellular and extracellular pressure, i.e., we assume the cell membranes are essentially flaccid. The myocardial fluid–fiber–collagen stress tensor has the same form proposed by Spencer (1972) for a fiber reinforced incompressible elastic material (Tözeren, 1986), and by Humphrey and Yin (1987) for finite deformations. Eq. 5 offers an important improvement over Eq. 1 in that the collagen resists a deformation perpendicular to the fiber direction, whereas the fluid–fiber continuum does not.

Analysis of Biaxial Loading of Passive Myocardial Tissue

The Young's moduli of the passive composite fiber (E) and of the collagen strut matrix (E_{cm}) determine the passive mechanical properties of the myocardium. These values can be found from experiments done on excised sheets of canine myocardium (Demer and Yin, 1983. Assuming that the collagen strut matrix is incompressible and isotropic, it follows that $E_{cm} = 3\mu_{cm}$. Thus the shear modulus (μ_{cm}) is proportional to the Young's modulus (E_{cm}) in such a medium. Since relatively thin slices of myocardium were used, the orientation of the fibers was approximately uniform. These sheets were submitted to uniaxial and biaxial loading in the predominant fiber direction and the cross-fiber direction. We apply the fluid–fiber–collagen stress tensor $\underline{\sigma}$ (Eq. 5) to the rectangular parallelopiped geometry shown in Fig. 3. We assume that the myocardial tissue is incompressible and we neglect viscoelastic and gravitational effects. Let the fibers be orientated along the y-axis (Fig. 3). On each edge of the sheet a uniform traction is exerted. We denote T_y and T_z as the tensile stresses exerted respectively in the y and z directions. No external traction is exerted in the x direction, but because of incompressibility $\epsilon_{xx} \neq 0$. Under this loading, the specimen deforms without shear strains ($\epsilon_{xy} = \epsilon_{xz} = \epsilon_{yz} = 0$). The three existing constant components of the strain tensor (ϵ_{xx}, ϵ_{yy}, and ϵ_{zz}) are determined as follows. The condition of local equilibrium ($\nabla \cdot \underline{\sigma} = \vec{0}$) yields P = constant. To determine the magnitude of P and the three constants of strain, the linearized tissue incompressibility constraint is required:

$$\epsilon_{xx} + \epsilon_{yy} + \epsilon_{zz} = 0, \tag{7}$$

as well as continuity of stress components on the bounding

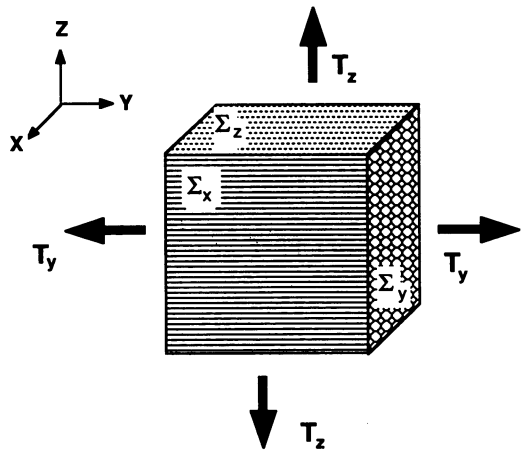

FIGURE 3 Geometry of myocardial sheet submitted to biaxial traction.

surfaces Σ_x, Σ_y, and Σ_z of the specimen (Fig. 3):

$$\sigma_{xx} = -P + 2\,\mu_{cm}\,\epsilon_{xx} = 0 \quad \text{on } \Sigma_x \tag{8a}$$

$$\sigma_{yy} = -P + T_f + 2\,\mu_{cm}\,\epsilon_{yy} = T_y \quad \text{on } \Sigma_y \tag{8b}$$

$$\sigma_{zz} = -P + 2\,\mu_{cm}\,\epsilon_{zz} = T_z \quad \text{on } \Sigma_z. \tag{8c}$$

The relationship between passive tension and fiber strain for the composite fiber ($\beta = 0$ in Eq. A2) is:

$$T_f = E\,\epsilon_f = E\,\epsilon_{yy}. \tag{9}$$

By substituting Eq. 9 into 8b, we obtain a linear system, Eqs. 7, 8a, 8b, and 8c for the unknowns (P, ϵ_{xx}, ϵ_{yy}, ϵ_{zz}). Two experiments must be analyzed. In one case, strains are not permitted in the cross fiber z-direction ($\epsilon_{zz} = 0$), and in the other strains are not permitted in the fiber y-direction, ($\epsilon_{yy} = 0$). For example, in the case with $\epsilon_{yy} = 0$, we find from Eq. 8c that $T_z = -P + 2\,\mu_{cm}\,\epsilon_{zz}$, but from Eqs. 8a and 7, $P = -2\,\mu_{cm}\,\epsilon_{zz}$, hence $T_z = 4\,\mu_{cm}\,\epsilon_{zz}$, or:

$$T_z = (4/3)\,E_{cm}\,\epsilon_{zz}. \tag{10}$$

Similarly, for the case $\epsilon_{zz} = 0$, we find:

$$T_y = [E + (4/3)\,E_{cm}]\,\epsilon_{yy}. \tag{11}$$

Eqs. 10 and 11 show that the modulus of elasticity measured in the fiber direction ($E + 4E_{cm}/3$) must be larger than the one measured in the cross-fiber direction ($4E_{cm}/3$).

For both cases, the full nonlinear relation measured during loading between stress and strain was fit by an exponential stress–strain relation that depended on three coefficients A, B, and C [stress = A exp (B strain) + C], (Demer and Yin, 1983, their Table I). For small strain, this stress–strain relation can be expanded in a series in powers of the strain [stress = $(A + C) + AB$-strain + $O(\text{strain}^2)$]. Table I indicates the elastic moduli of the passive composite fiber E and the collagen strut matrix E_{cm} as derived from the linear component (AB) of the elastic parameters previously fit (Demer and Yin, 1983) for a series of isometric uniaxial tests. The two values of the Young's moduli, $E_{cm} \approx 3.41 \pm 0.62 \times 10^5$ dyn/cm^2 and $E \approx 3.93 \pm 1.02 \times 10^5$ dyn/cm^2, have the same order of magnitude. So, it is clear that for small strain and during passive state of the myocardium the collagen strut matrix considerably affects the mechanical properties of the left ventricular wall. This corroborates a criticism (Fung, 1984) that the passive myocardium is not as anisotropic as the fluid–fiber model (Eq. 1) originally suggested.

It is interesting to calculate how the myocardial tissue pressure would change in these experiments. For example corresponding to the case for which Eq. 10 was derived, we find $P = -(2/3)\,E_{cm}\,\epsilon_{zz}$. Taking $\epsilon_{zz} = 0.1$, and $E_{cm} = 3.4 \times 10^5$ dyn/cm^2, we find $P \approx -17$ mmHg. To explain the negative tissue pressure we note that a positive strain in the cross-fiber z-direction implies a compressive strain across the specimen thickness in the x-direction due to tissue incompressibility. Hence, to have zero normal stress on the unloaded face (Σ_x), a negative tissue pressure is required to counteract the outward push of the collagen strut matrix.

TABLE I
ELASTIC MODULI OF THE PASSIVE COMPOSITE FIBER E AND OF THE COLLAGEN MATRIX E_{cm}

Specimen	Unit (g/cm^2)			
	AB (fiber direction)	AB (cross-fiber direction)	E	E_{cm}
310*	317.3*	420.4*	*	*
317	295.8	263.6	32.2	197.7
318	1547.7	686.5	861.2	514.9
324*	711.1*	1227.4*	*	*
407	604.6	326.8	277.8	245.1
422	1129.5	778.5	351	583.9
423	845.6	514.1	331.5	385.6
602*	57.8*	330.5*	*	*
609*	708.8*	1036.5*	*	*
623	829.6	416.2	413.4	312
701	799.5	260.8	538.7	195.6
Mean (g/cm^2)	864.6 ± 161.0	463.8 ± 83.9	400.8 ± 104.0	347.8 ± 62.9
($\times 10^5$ dyn/cm^2)	8.48 ± 1.58	4.55 ± 0.82	3.93 ± 1.02	3.41 ± 0.62

Table entrees with an asterisk had a larger cross-fiber stiffness than parallel fiber stiffness, and were not included in the determination of the mean values. Values represent the loading portion of the cycle only. (Adapted from experimental results of Demer and Yin, 1983.)

Effects on the Mechanics of the Left Ventricle

Some experimental results (Robinson et al., 1986) have suggested that collagen tissue may play an important role in the mechanism of the LV filling, by storing energy from contraction during systole as elastic energy to provide the potential energy for a suction that aids filling. In order to investigate this hypothesis, we extend our previous work done on the mechanics of the LV (Chadwick, 1981, 1982; Pelle et al., 1984; Ohayon et al., 1987; and Ohayon and Chadwick, 1987) by including the effect of this connective tissue in our model.

Equations of the Model. A detailed description of the mathematical model is given elsewhere (Chadwick, 1982). The basic assumptions and equations used in the LV model are given in the Appendix.

The continuity of normal stress components on the endocardial (Σ_{endo}, or on $\rho = 1$) and on the epicardial (Σ_{epi}, or on $\rho = \alpha$) surfaces are:

$$P(\rho, t) = P_v(t) + 2\mu_{cm}\,\epsilon_{\rho\rho}(\rho, t) \quad \text{on } \rho = 1; \tag{12a}$$

$$P(\rho, t) = 2\mu_{cm}\,\epsilon_{\rho\rho}(\rho, t) \quad \text{on } \rho = \alpha, \tag{12b}$$

where P_v is the LV cavity pressure. Note that in these two boundary conditions, there is no contribution from the fiber stress since the assumed fiber direction ($\vec{\tau}$) is perpendicular to the radial direction (Eq. A1). For this condition, Eq. 5 shows that the radial component of the stress tensor is not affected by the presence of the fibers. However, because of the presence of the collagen strut matrix in the myocardial tissue, the tissue pressure is not continuous across the endocardial ($\rho = 1$) and epicardial ($\rho = \alpha$) surfaces. At each instant of time during the cardiac cycle, the LV structure is assumed to be in a state of mechanical equilibrium. The local equilibrium equation is $\nabla \cdot \underline{\sigma} = \vec{0}$, or:

$$\nabla P = \mu_{cm} \nabla^2 \vec{u} + \vec{\tau}(T_f \nabla \cdot \vec{\tau} + \vec{\tau} \cdot \nabla T_f) + T_f(\vec{\tau} \cdot \nabla)\vec{\tau}. \quad (13)$$

The displacement field $\vec{u}$ satisfying the incompressibility condition $\nabla \cdot \vec{u} = 0$, given in the Appendix happens also to be harmonic so that $\nabla^2 \vec{u} = \vec{0}$. Since the problem is axisymmetric, all terms involving theta derivatives (circumferential coordinate) vanish. So, the circumferential component of the equilibrium equation implies $\partial T_f/\partial z = 0$ which then implies, by using the axial component of the equilibrium equation, that $\partial P/\partial z = 0$. Therefore P and T_f are functions of the radial coordinate only. So, the radial component of the equilibrium equation reduces to:

$$\frac{\partial P(\rho, t)}{\partial \rho} = -\frac{T_f(\rho, t)}{\rho} \cos^2\gamma(\rho) \quad (14a)$$

or its radially integrated form:

$$P(\rho, t) = P(\alpha, t) + \int_\rho^\alpha T_f(\rho, t) \cos^2\gamma(\rho) \frac{d\rho}{\rho}. \quad (14b)$$

The normal state of deformation of the structure includes torsion of the cylinder due to the rotation of the apex, which is free to rotate with respect to the assumed fixed base. Global static equilibrium requires that the net vertical force and moment acting on the apical surface of the cylinder are zero, these equations are given respectively by:

$$P_v(t) = 2 \int_1^\alpha \cdot [T_f(\rho, t) \sin^2\gamma(\rho) + 2\mu_{cm} \epsilon_{zz}(t) - P(\rho, t)]\rho \, d\rho; \quad (15a)$$

$$0 = \int_1^\alpha [T_f(\rho, t) \cos\gamma(\rho) \sin\gamma(\rho) + 2\mu_{cm} \epsilon_{\theta z}(\rho, t)]\rho^2 \, d\rho. \quad (15b)$$

Integrating the last term of Eq. 15a by parts and using the differential expression of the local equilibrium condition Eq. 14a, the continuity of normal stresses on the endocardial and epicardial surfaces Eqs. 12a and 12b, and the component of the displacement field Eq. A3, the vertical equilibrium of the bottom plate Eq. 15a can also be expressed as:

$$0 = 3\mu_{cm}(\alpha^2 - 1)\epsilon_{zz}(t) + \int_1^\alpha T_f(\rho, t) [2 \sin^2\gamma(\rho) - \cos^2\gamma(\rho)] \, \rho d\rho. \quad (16)$$

Eqs. A2, A3, A4, 12, 14b, 15a, and 16 are fundamental relations for the model of left ventricular mechanics and determine the state of deformation, the stress field, and the activation function when ventricular pressure and volume are specified as a function of time. With simultaneous activation of fibers, this system constitutes a coupled algebraic system for $\beta(t)$, $C_1(t)$, and $\theta_0(t)$. Once these quantities are determined the transmural distributions of fiber strain, fiber stress, and myocardial tissue pressure can be calculated.

Pressure–Volume Relation. The global mechanics of the left ventricle is represented by the left ventricular pressure–volume relationship. This relationship is useful to study the interaction of the LV with the systemic circulation, or for estimation of the elastic parameters (E, μ_{cm}, E^*, T_0) from pressure–volume data.

Our theory predicts a pressure–volume relationship that has the form of a linear time-varying elastance model as was found experimentally by Sagawa (1978):

$$P_v(t) = \mathcal{E}(t) \, [V(t) - V_d(t)]. \quad (17a)$$

The elastance $\mathcal{E}(t)$ and zero pressure volume $V_d(t)$ can be expressed in terms of functions that we tabulated for convenience:

$$\mathcal{E}(t) = \frac{E_f(t)}{2 V_0}\left[\frac{f_1 + \xi(t) f_2 + \xi(t)^2 f_3 + \xi(t)^3 f_4}{h_1 + \xi(t) h_2 + \xi(t)^2 h_3}\right]; \quad (17b)$$

$$V_d(t) = V_0 - \frac{2 V_0 \beta T_0}{E_f(t)}\left[\frac{g_1 + \xi(t) g_2 + \xi(t)^2 g_3}{f_1 + \xi(t) f_2 + \xi(t)^2 f_3 + \xi(t)^3 f_4}\right], \quad (17c)$$

where

$$\xi(t) = \mu_{cm}/E_f(t), \quad (17d)$$

and

$$f_4 = \frac{3}{2\alpha^2}(\alpha^2 - 1)^3 (\alpha^2 + 1), \quad (17e)$$

and

$$h_3 = \frac{3}{4}(\alpha^2 - 1)^2 (\alpha^2 + 1). \quad (17f)$$

The functions $f_1, f_2, f_3, g_1, g_2, g_3, h_1$, and h_2 depend on the geometrical parameters α and γ_0, and are tabulated in Table II. The two linear $P_v(t) - V(t)$ relationships at end diastole ($\beta = 0$) and end systole ($\beta = 1$) can be easily obtained from these last equations. $V_d(t)$ at end diastole is equal to the unstressed volume V_0 of the relaxed ventricle and it becomes minimal at end systole. Note that for a fluid–fiber myocardium ($\xi(t) = 0$), we obtain from Eq. 17, the same end-diastolic and end-systolic pressure–volume lines presented by Chadwick (1982).

TABLE II
FUNCTION TABULATIONS FOR PRESSURE–VOLUME RELATION

$f_1(\alpha, \gamma_0)$

	γ_0				
α	50°	60°	70°	80°	90°
1.2	0.000	0.000	0.000	0.000	0.000
1.4	0.001	0.001	0.002	0.002	0.002
1.6	0.003	0.005	0.008	0.009	0.009
1.8	0.009	0.015	0.020	0.023	0.024
2.0	0.021	0.033	0.044	0.050	0.052

$f_2(\alpha, \gamma_0)$

	γ_0				
α	50°	60°	70°	80°	90°
1.2	0.006	0.007	0.007	0.008	0.008
1.4	0.059	0.064	0.067	0.070	0.071
1.6	0.234	0.249	0.260	0.268	0.271
1.8	0.651	0.683	0.707	0.724	0.728
2.0	1.488	1.541	1.579	1.607	1.611

$f_3(\alpha, \gamma_0)$

	γ_0				
α	50°	60°	70°	80°	90°
1.2	0.072	0.072	0.072	0.072	0.072
1.4	0.666	0.664	0.662	0.660	0.659
1.6	2.620	2.607	2.594	2.581	2.573
1.8	7.266	7.213	7.157	7.105	7.070
2.0	16.587	16.427	16.255	16.100	15.995

$g_1(\alpha, \gamma_0)$

	γ_0				
α	50°	60°	70°	80°	90°
1.2	0.000	0.000	0.000	0.000	0.001
1.4	0.002	0.003	0.004	0.005	0.005
1.6	0.007	0.013	0.018	0.022	0.023
1.8	0.022	0.039	0.055	0.065	0.068
2.0	0.056	0.096	0.134	0.158	0.166

$g_2(\alpha, \gamma_0)$

	γ_0				
α	50°	60°	70°	80°	90°
1.2	0.008	0.009	0.009	0.008	0.008
1.4	0.086	0.093	0.094	0.090	0.085
1.6	0.387	1.417	0.416	0.399	0.376
1.8	1.200	1.286	1.278	1.218	1.144
2.0	3.022	3.225	3.188	3.023	2.827

TABLE II (cont.)

$g_3(\alpha, \gamma_0)$

	γ_0				
α	50°	60°	70°	80°	90°
1.2	0.050	0.046	0.041	0.036	0.032
1.4	0.537	0.485	0.433	0.385	0.342
1.6	2.380	2.147	1.915	1.698	1.510
1.8	7.292	6.572	5.855	5.188	4.609
2.0	18.148	16.340	14.541	12.868	11.419

$h_1(\alpha, \gamma_0)$

	γ_0				
α	50°	60°	70°	80°	90°
1.2	0.002	0.002	0.003	0.004	0.005
1.4	0.010	0.013	0.019	0.025	0.029
1.6	0.032	0.043	0.060	0.078	0.090
1.8	0.079	0.105	0.146	0.188	0.218
2.0	0.170	0.223	0.306	0.392	0.454

$h_2(\alpha, \gamma_0)$

	γ_0				
α	50°	60°	70°	80°	90°
1.2	0.061	0.069	0.076	0.081	0.085
1.4	0.356	0.401	0.438	0.467	0.489
1.6	1.143	1.284	1.397	1.483	1.551
1.8	2.838	3.178	3.445	3.645	3.800
2.0	6.066	6.776	7.319	7.716	8.022

Numerical Results. We present calculated results that show the effects of the isotropic collagen matrix on the mechanics of the LV, by fitting the fluid–fiber model and the fluid–fiber–collagen model to the same pressure and volume waveforms shown in Fig. 4. To be consistent, the myocardial volume (V_m) must be the same in the two models.

$$V_m = V_0 (\alpha^2 - 1) = \text{constant}. \quad (18)$$

When the mechanical properties of the myocardium are changed by introducing the collagen, the elastance of the ventricle, $\mathcal{E}(t)$ (Eq. 17b), increases and the ventricle has a

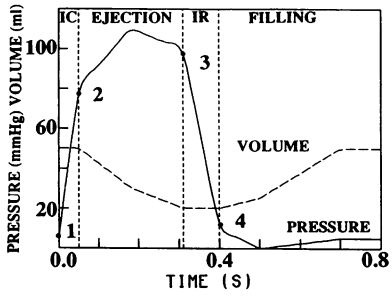

FIGURE 4 Pressure and volume input data waveforms used in computations.

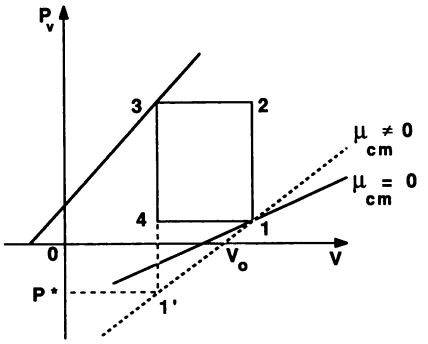

FIGURE 5 Pressure–volume loop and filling index P^*. Collagen struts ($\mu_{cm} \neq 0$) decrease P^*.

steeper end-diastolic line. For the two models the end-diastolic point in the P_v–V plane is fixed, and to maintain constant V_m, new values of α and V_0 must be computed. To maintain the contractility (end-systolic pressure–volume line) and the end-systolic P_v–V point fixed, new values of E^* and T_0 must also be computed. Fig. 5 illustrates the change in slope of the end-diastolic line, the change in V_0, and the constancy of the end-systolic line.

The results presented here were obtained for the following values for the fluid–fiber model: $E = 2 \times 10^5$ dyn/cm^2; $\gamma_0 = 70°$; $R_i/L_0 = 0.324$ (inner radius/length of the ventricle at unloaded diastole); $E^* = 25 \times 10^5$ dyn/cm^2; $T_0 = 6.3 \times 10^5$ dyn/cm^2; $V_0 = 32.7$ ml and $\alpha = 1.6$. When collagen is introduced ($E_{cm} = 1.7 \times 10^5$ dyn/cm^2), we calculate $E^* = 35 \times 10^5$ dyn/cm^2, $T_0 = 10.5 \times 10^5$ dyn/cm^2, $V_0 = 43.4$ ml, and $\alpha = 1.46$. Somewhat smaller values of the passive elastic moduli were needed than were determined in Table I, which overestimate the cycle average of loading and unloading. Fig. 6 shows that the effect of the collagen tends to equalize the transmural distribution of the composite fiber strain during the cardiac cycle and limit muscle fiber lengthening at end diastole. Note that

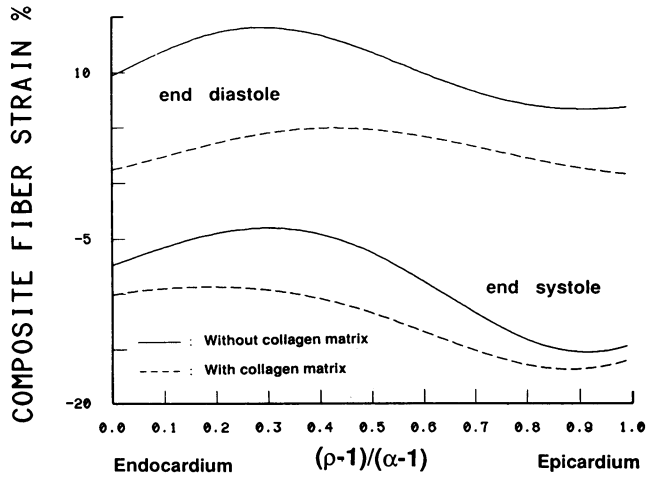

FIGURE 6 Effect of collagen strut matrix on the transmural distribution of fiber strain.

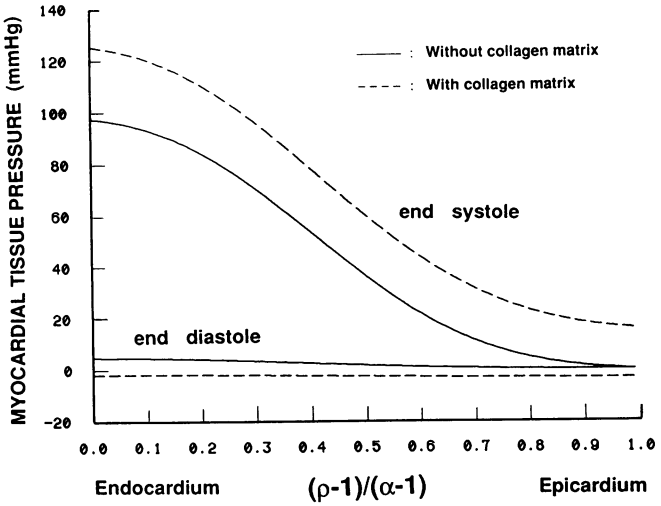

FIGURE 7 Effect of collagen strut matrix on the transmural distribution of tissue pressure.

the myocardial tissue pressure at the subendocardial layers exceeds the ventricular pressure at the end-systolic state (Fig. 7), whereas the opposite is true during end diastole.

The increase of collagen density in the myocardium is related to an increase in the Young's modulus of the collagen strut matrix E_{cm}. To better understand the effect of the proportion of collagen on the ventricular performance, we do the following simulation. Maintaining the end-systolic and end-diastolic LV pressures, the rheological properties of the cardiac fibers, and the geometrical parameters of the model constant, the results (Table III) show that, when E_{cm} increases, the passive elastance of the ventricle increases faster than the active elastance (columns 2 and 3, Table III), and the ejection fraction (EF) and the stroke volume (SV) both decrease (columns 4 and 5, Table III).

Elastic Energy Storage in the Myocardium

Negative cavity pressures can occur when filling is prevented. We investigate the effect of the collagen strut matrix on that process by simulating a closed mitral valve during the diastolic phase. This forces the ventricle to continue its isovolumic relaxation phase until the passive state (1') shown in Fig. 5. During this phase, the ventricu-

TABLE III
EFFECT OF ELASTIC MODULUS OF COLLAGEN STRUT MATRIX ON END-DIASTOLIC ELASTANCE ($\mathcal{E}_{ed}$) END-SYSTOLIC ELASTANCE ($\mathcal{E}_{es}$), STROKE VOLUME (SV), AND EJECTION FRACTION (EF)

E_{cm}	$\mathcal{E}_{ed}$	$\mathcal{E}_{es}$	SV	EF
dyn/cm^2	*mmHg/ml*	*mmHg/ml*	*ml*	
1.7×10^5	0.725	3.973	30.246	0.602
3.4×10^5	1.244	4.535	24.338	0.514
5.1×10^5	1.762	5.084	20.869	0.452

lar pressure decreases and becomes negative (provided the end-systolic volume is less than V_0) to reach the minimum P^* at the intersection with the end-diastolic P_v–V line. This pressure (P^*) is the minimal achievable P_v and serves as an index of the importance of the stored elastic energy in the myocardium. The computations with collagen give $P^* = -17.4$ mmHg, and without collagen, $P^* = -3.6$ mmHg. In both cases the calculation of P^*, with ($\xi \neq 0$) and without ($\xi = 0$) the collagen strut matrix, is obtained from Eq. 17 with $\beta = 0$ and $V(t)$ equal to end-systolic volume. Thus, we show that the collagen provides a mechanism for greater storage and release of elastic energy and hence a greater potential for diastolic suction to aid filling. The experimental results of Yellin et al. (1986) on anesthetized dogs show that, in the isovolumic nonfilling cycle induced by occluding the mitral valve at end systole, the LV relaxes to a pressure minimum P^* in the range of -7.3 ± 3.3 mmHg. Even more negative values were reported by Tyberg et al. (1970). The larger calculated suction pressure can be partially explained by unavoidable flow from Thebesian drainage in the experiments.

In order to compare the elastic strain energy stored by the collagen strut matrix with that stored by the collagen sheath, we compute the strain energy stored in the passive constituents of the myocardium at the end-systolic state:

$$W = \int \sigma_{ij}\, d\epsilon_{ij} = E \int \epsilon_f\, d\epsilon_f + 2\mu_{cm} \int \epsilon_{ij}\, d\epsilon_{ij}, \qquad (19)$$

where the limits of integration (in Eq. 19) are from the zero strain reference state to the strain level at state 3 of Fig. 5. This computation was done with and without the presence of the collagen strut matrix in the myocardium. The second term of the right expression of Eq. 19 represents the energy stored by the collagen strut matrix and the first term is the energy stored by the passive elements of the composite fiber (collagen sheath, Z lines of the sarcomeres, etc). It appears from the results (Fig. 8) that: (*a*) the collagen strut matrix stores more energy than the collagen sheath (curves 1 and 2); (*b*) the energy stored by the myocardium with the collagen strut matrix is larger than without the collagen strut matrix (curves 3 and 4); (*c*) the energy stored by the collagen strut matrix is maximal in the subendocardial layers (curve 1); and (*d*) the energy stored by the passive elements of the composite fiber is maximal in the subepicardial layers (curves 4 and 2). These results are consistent with experiments (Robinson et al., 1986) illustrating the more efficient filling of mammalian hearts compared to amphibian hearts, where the former have a denser collagen strut matrix.

Effective Elasticity of the Composite Fiber

The relationship between the effective Young's modulus of one composite fiber (E'_f), the modulus of one muscle fiber (E'_{mf}), and the modulus of a fiber in the collagen sheath (E_{cf}) is investigated, under the assumption that the collagen sheath remains in contact with the muscle fiber. The total work required to stretch the composite fiber (W_f) is equal to the work used to stretch the muscle fiber (W_{mf}) plus the work used to stretch all helicoidal collagen fibers in the sheath (W_{cs}):

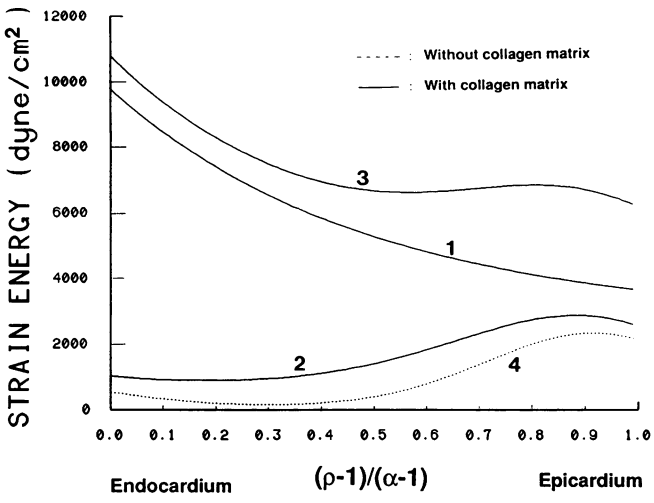

FIGURE 8 Transmural distribution of passive elastic strain energy stored in collagen at end-systole. Curve *1*, energy stored in struts; curve *2*, energy stored in sheaths; curve *3*, energy stored in struts and sheaths; curve *4*, energy stored in passive elements of composite fiber when no struts are present.

$$W_f = W_{mf} + W_{cs}. \qquad (20)$$

We use Eq. 20 to derive the effective Young's modulus of the composite fiber. The expression for the total work is given by:

$$W_f = \frac{1}{2} E'_f A_f L \epsilon_{zz}^2, \qquad (21)$$

where A_f, L, and ϵ_{zz} are respectively the total cross-sectional area, the reference length, and the axial strain of the composite fiber. For convenience, let L be chosen equal to the axial pitch of the helicoidal collagen fibers. The work used to stretch only the muscle fiber is:

$$W_{mf} = \frac{1}{2} E'_{mf} A_{mf} L \epsilon_{zz}^2, \qquad (22)$$

where A_{mf} is the cross-sectional area of the muscle fiber. Let n be the total number of helicoidal collagen fibers on a circumference that form the sheath of collagen, then the work used to stretch the sheath is:

$$W_{cs} = \frac{1}{2} n E_{cf} A_{cf} L_f \epsilon_{cf}^2, \qquad (23)$$

where A_{cf}, L_f, and ϵ_{cf} are respectively the cross-sectional area, the initial length, and the strain of the collagen fiber. Let ψ be the inclination of the helicoidal collagen fiber with respect to the equatorial plane of the muscle fiber (Fig. 9).

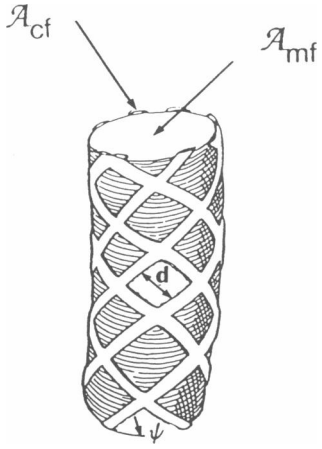

FIGURE 9 Schematic showing geometrical parameters of composite fiber.

Its initial length is also expressed as:

$$L_f = \frac{L}{\sin\psi}. \tag{24}$$

The expression of the collagen fiber strain ϵ_{cf} depends on the circumferential ($\epsilon_{\theta\theta}$) and axial (ϵ_{zz}) strain of the muscle fiber:

$$\epsilon_{cf} = \epsilon_{\theta\theta}\cos^2\psi + \epsilon_{zz}\sin^2\psi. \tag{25}$$

Assuming that the muscle fiber is incompressible, undergoes axisymmetric deformation, and keeps its assumed cylindrical shape during deformation, the relationship between the principal strains are:

$$\epsilon_{zz} = -2\,\epsilon_{\theta\theta} = -2\,\epsilon_{rr}, \tag{26}$$

where ϵ_{rr} is the radial strain. Substituting Eqs. 24, 25, and 26 into Eq. 23, then substituting Eqs. 21, 22, and 23 into Eq. 20, we obtain the effective Young's modulus of the composite fiber:

$$E'_f = \frac{1}{A_f}\left[A_{mf}E'_{mf} + \frac{n}{4\sin\psi}A_{cf}(2\sin^2\psi - \cos^2\psi)^2 E_{cf}\right]. \tag{27}$$

The number of collagen fibers (n) on a circumference of the muscle fiber can be expressed in terms of the radius of the muscle fiber (R_{mf}), the perpendicular distance between the centers of two adjacent collagen fibers (d), and the pitch angle of the weave (ψ):

$$n = 2\left(\frac{2\pi R_{mf}}{d}\sin\psi\right). \tag{28}$$

Note that the first factor of two in Eq. 28 is due to the superposition of two networks of parallel fibers of collagen of opposite angular orientation with the respect of equatorial plane. Substituting Eq. 28 into Eq. 27, the effective modulus of the composite fiber can also be expressed as:

$$E'_f = \frac{A_{mf}}{A_f}\left[E'_{mf} + \frac{A_{cf}}{R_{mf}\,d}f(\psi)\,E_{cf}\right] \tag{29}$$

with

$$f(\psi) = (2\sin^2\psi - \cos^2\psi)^2. \tag{30}$$

It is clear from Eq. 29 that the modulus of the composite fiber E'_f depends strongly on the pitch angle of the collagen weave (ψ). This dependence is introduced by the geometrical function $f(\psi)$ given in Eq. 30. This function is plotted in Fig. 10 and is seen to be non-negative. It appears that, for one particular pitch angle of the network ($\psi = \tan^{-1}(1/\sqrt{2}) \approx 35.3°$), the collagen weave has no effect on the elastic properties of the composite fiber ($f(\psi) = 0$). For that particular orientation, we have no strain of the collagen fibers ($\epsilon_{cf} = 0$). This possibility is related to the incompressibility of the muscle fiber. When the composite fiber is extended for example, the length of the helicoidal collagen fibers tends to increase with the increased length of the composite fiber, but also tends to decrease with the reduced radius of the composite fiber resulting from incompressibility. So, for this pitch angle of the weave, the combination gives zero strain of the collagen fibers. Note that due to the incompressibility condition, a network comprised only of circumferential collagen fibers ($\psi = 0°$) also affects the elasticity of the composite fiber (Fig. 10). The maximal effect is observed for $\psi = 90°$, when the collagen is aligned along the axis of the muscle fiber.

The relative contributions of the passive elastic elements in the muscle fiber and the collagen sheath to the passive elastic modulus of the composite fiber can be obtained in principle from Eq. 29. Unfortunately, a diversity of experimental techniques is required to critically test this relationship. Quantitative ultrastructural studies are needed to determine the geometrical factors, and the elastic moduli must be determined for both an unskinned and skinned cardiac fiber.

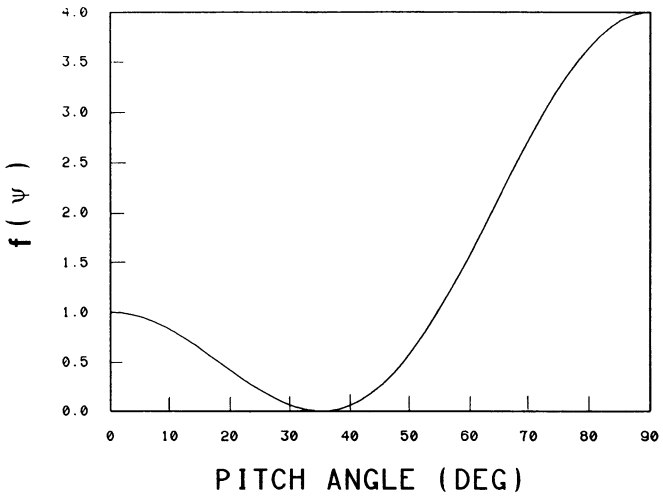

FIGURE 10 Helix angle function $f(\psi)$ given in Eq. 30.

DISCUSSION

The concept of myocardial tissue pressure as introduced in the subsection Continuum Stress Tensor for the Myocardium requires further comment with regards to whether or not such pressure has a physical meaning, its measureability, and its relation to the concept of tissue fluid pressure introduced by Bogen (1987).

The suggestion and confusion that tissue pressure may not be a physical entity can be traced to the use of minimization of elastic strain energy to derive the equations for elastic equilibrium. In the case of an incompressible elastic material, the incompressibility constraint is introduced into the strain energy function via an arbitrary Lagrange multiplier. After minimization, the arbitrary Lagrange multiplier appears in the equations of equilibrium in the form of an isotropic stress that can be identified as a hydrostatic pressure.

There are possibly three sources of confusion: the term "arbitrary," the term "Lagrange multiplier," and the concept of hydrostatic pressure in a solid. In fact, the arbitrariness is only temporary. The Lagrange multiplier can be completely determined from the solution of the equations of equilibrium and the boundary conditions. Nevertheless, the "stigma" of the mathematical term, "Lagrange multiplier," remains and gives the aura of unreality. Exactly the same situation arises in incompressible fluids, but without the aura of unreality. The dynamic equations for the motion of an inviscid, incompressible fluid can be derived from Hamilton's principle. The incompressibility constraint is introduced into the energy function via an arbitrary Lagrange multiplier, which also appears in the equations of motion after the variational process (Sommerfeld, 1950). However, the confusion about the Lagrange multiplier being identified with pressure in a fluid and having a physical meaning does not usually arise.

The different conceptions in the fluid and solid case are evidently tied to the ease of measureability. Pressure in a fluid is routinely measured, whereas the measurement of hydrostatic pressure in a solid is technically very difficult. Ease of measurability should not be regarded as a determinant of physical reality. Likewise the myocardial tissue pressure introduced and calculated in the present work has a physical meaning, even though it may be difficult to measure. Our argument is based on the idea that it represents the continuum approximation to certain stresses existing in the fluid and collagen components that directly act on adjacent structures, such as small intramyocardial blood vessels, etc. Heineman and Grayson (1985) have measured pressure inside the beating myocardium using a sophisticated servocontrolled micropipette device. Does that transducer measure myocardial tissue pressure as defined here? We feel that it does not determine the full tissue pressure, but only the hydrostatic component since the transducer has an open end. However, a transducer with an end closed by a large enough spherical capsule (but small enough not to cause significant tissue distortion) would sense the isotropic component of both fluid and collagen, and hence the full tissue pressure.

Bogen (1987) introduced a method to calculate tissue fluid pressure in swelled isotropic tissue. During swelling with no external work on the boundaries, he found the pressure can be calculated as the derivative of that part of the strain energy not involving the incompressibility constraint, with respect to the volumetric dilatation. To make that more explicit let:

$$W = W_c + W_{el}, \tag{31}$$

where W is the total strain energy, W_c is that part due to incompressibility constraint, and W_{el} is the remaining elastic part. According to Bogen:

$$P = \frac{dW_{el}}{de}, \tag{32}$$

where e is the volumetric dilatation. In terms of the small deformation analysis used here,

$$e = \epsilon_{xx} + \epsilon_{yy} + \epsilon_{zz}. \tag{33}$$

If we specialize the strain energy function (Eq. A6) for the case of no fibers and zero shear, then

$$W_{el} = \mu_{cm}(\epsilon_{xx}^2 + \epsilon_{yy}^2 + \epsilon_{zz}^2). \tag{34}$$

For isotropic swelling $\epsilon_{xx} = \epsilon_{yy} = \epsilon_{zz} = \epsilon$, and $e = 3\epsilon$, so that:

$$W_{el} = \frac{1}{3}\mu_{cm}\, e^2. \tag{35}$$

Then from Eq. 32 we calculate

$$P = \frac{2}{3}\mu_{cm}\, e. \tag{36}$$

Alternatively, we can determine the myocardial tissue pressure directly from continuity of normal stress acting on the face of a small cubical element to obtain the same result:

$$\sigma_{xx} = \sigma_{yy} = \sigma_{zz} = 0 = -P + 2\mu_{cm}\epsilon \tag{37}$$

or

$$P = 2\mu_{cm}\epsilon = \frac{2}{3}\mu_{cm}\, e.$$

Thus we can conclude that the myocardial tissue pressure introduced in this paper is identical with that calculated using Bogen's method. It should be pointed out, however, that for swelling of anisotropic tissue, or for constant volume deformations, the equations of equilibrium and boundary conditions must be used to determine the tissue pressure. It is also interesting to mention that Eq. 32 is equivalent to the statement that $dW = 0$ for free adiabatic swelling. From Eq. A6, $W_c = (-P_h + \lambda_{cm}e/2)e$,

so $dW = (-P_h + \lambda_{cm}e + 2\mu_{cm}e/3)\,de = 0$. Taking the limit $\lambda_{cm} \to \infty$, $e \to 0$, and remembering

$$P = P_h - \lim_{\substack{\lambda_{cm} \to \infty \\ e \to 0}} \lambda_{cm} e,$$

we recover Eqs. 36 and 37.

Throughout this work we have used a linear analysis to approximate the behavior of the myocardium and the left ventricle. We feel that this approach may not be as restrictive as is commonly believed. It is very difficult to eliminate gross sarcomere length nonuniformity due to ischemia and mechanical damage in preparations used to determine the stress–strain relations in cardiac tissue. Because of the series arrangement of sarcomeres, the strain-hardening behavior of the gross passive tissue may be exaggerated by overstretched sarcomeres. Elimination of these effects tends to extend the linear range of the passive muscle. The experiments of ter Keurs et al. (1980) on trabeculae from the rat right ventricle show that the linear range of the passive stress–strain relation is extended to 20% strain, which is larger than our calculated operating range. In that preparation ends were not damaged, the small diameter insured sufficient oxygenation, and the sarcomere length was servocontrolled. Furthermore, the active stress–strain relations were linear provided the extracellular Ca^{2+} levels did not saturate the response.

The small deformation approximation has also been used in this study. The calculated fiber strains of <20% are consistent with the measurements of Printzen et al. (1986) on open-chested dogs. Though it is possible to carry out a finite deformation analysis on the cylindrical model (Tözeren, 1983), we felt any quantitative improvement in accuracy would be offset by the uncertainty in the reference configuration, and limitations of the cylindrical geometry itself. For those reasons we have concentrated on developing linear mathematical techniques that can be readily applied to more realistic geometries and corrected for finite deformations using perturbation techniques.

APPENDIX

Model for the Mechanics of the Left Ventricle

A linear theory is used to describe the mechanics of the LV. The geometry of the LV is taken as a finite thick-walled cylinder. The upper surface or base (at $z = 0$) is assumed to be fixed. On this surface radial displacements are allowed, but axial and circumferential displacements are zero. The bottom surface or apex (at $z = -L_0$) is assumed to be a free plane which can translate vertically and twist as a rigid body about the axis of the cylinder. Radial displacements are allowed to occur to maintain the cylindrical shape.

The myocardium is considered as a fluid–fiber–collagen continuum described by the constitutive law given in Eq. 5. The fiber direction field in cylindrical coordinates (ρ, θ, z) is taken as:

$$\vec{\tau} = \cos\gamma(\rho)\vec{e}_\theta + \sin\gamma(\rho)\vec{e}_z. \tag{A1}$$

Thus, the fibers form regular helices on cylindrical surfaces. The fiber inclination angle $\gamma(\rho)$ (relative to the equatorial plane) varies linearly across the wall from $\gamma_0 = -70°$ at the epicardium to $\gamma_0 = 70°$ at the endocardium (Streeter, 1979).

The relationship between composite fiber tension T_f and strain ϵ_f is approximated by a linear relationship (Chadwick, 1982), both in the passive state (characterized by the elastic modulus E), and the maximally active state (characterized by the elastic modulus E^* and active tension at zero strain, T_0). During the cardiac cycle the composite fiber rheological behavior is represented by a linear combination of these two states using the time-dependent activation function $\beta(t)$; $(0 \le \beta \le 1)$:

$$T_f = E_f(t)\epsilon_f + \beta T_0 \text{ with } E_f(t) = (1 - \beta)\,E + \beta E^*. \tag{A2}$$

The reference unstressed LV configuration is defined during the passive state at zero transmural pressure (zero epicardial pressure is assumed). In this state the sarcomere length is assumed to be 1.9 μm (Feit, 1979). Inertial, gravitational, viscoelastic, and transmural delay in activation effects are neglected.

A cylindrical model with anisotropic fibrous material can expand both circumferentially and longitudinally and can also rotate around its axis. By assuming axisymmetry, the pressure, tension, and fiber strain are functions of time (t) and a normalized radial coordinate $\rho = R/R_i$ $(1 \le \rho \le \alpha)$ only, where α is the ratio of outer (R_o) to inner (R_i) radius in the reference state. A displacement field $\vec{u}(\rho, z, t)$ can be derived in cylindrical coordinates, that satisfies the tissue incompressibility constraint in the limit of infinitesimal strain (Chadwick, 1981):

$$\begin{aligned} u_\rho &= R_i[-(1/2)C_1(t)\rho + C_2(t)/(R_i^2\rho)]; \\ u_\theta &= -z\rho R_i\theta_o(t)/L_0; \\ u_z &= C_1(t)z, \end{aligned} \tag{A3}$$

where L_0 is the length of the cylinder in the reference configuration and $C_1(t)$, $C_2(t)$, and $\theta_o(t)$ are arbitrary functions of time. $C_1(t)$ is the axial strain, $\theta_o(t)$ is the twist angle of the bottom plane located at $z = -L_0$, and $C_2(t)$ is related to volumetric strain (cf. Eq. A5). When viewed from the apex, a clockwise rotation defines the sense of positive θ_o. The infinitesimal strain of the composite fiber is expressible as a function of the known linear radial distribution of the helicoidal pitch angle $\gamma(\rho)$ and the displacement components (u_ρ, u_θ, u_z) given by Eqs. (A3):

$$\epsilon_f = [(\vec{\tau} \cdot \nabla)\vec{u}] \cdot \vec{\tau}. \tag{A4}$$

In the small deformation theory the condition of conservation of myocardial volume leads to the following expression that relates the chamber volume $V(t)$ to the volumetric strain $C_2(t)$:

$$V(t) = V_o[1 + 2C_2(t)/R_i^2], \tag{A5}$$

where V_o is the volume of the cylinder in the reference configuration.

The constitutive relation for cardiac tissue, Eq. 5, can also be formulated in terms of a strain energy function W expressed in cartesian coordinates (x, y, z):

$$\begin{aligned} W = {} & (-P_h + \lambda_{cm}e)e/2 + \mu_{cm}(\epsilon_{xx}^2 + \epsilon_{yy}^2 + \epsilon_{zz}^2) \\ & + 2\mu_{cm}(\epsilon_{xy}^2 + \epsilon_{xz}^2 + \epsilon_{yz}^2) \\ & + (\beta T_o/2)[\tau_x^2\epsilon_{xx} + \tau_y^2\epsilon_{yy} + \tau_z^2\epsilon_{zz} \\ & + 2(\tau_x\tau_y\epsilon_{xy} + \tau_x\tau_z\epsilon_{xz} + \tau_y\tau_z\epsilon_{yz})] \\ & + (E_f/2)[\tau_x^2\epsilon_{xx} + \tau_y^2\epsilon_{yy} + \tau_z^2\epsilon_{zz} \\ & + 2(\tau_x\tau_y\epsilon_{xy} + \tau_x\tau_z\epsilon_{xz} + \tau_y\tau_z\epsilon_{yz})]^2. \end{aligned} \tag{A6}$$

The authors are very grateful for useful discussions with Dr. F. C. P. Yin, Department of Medicine, Johns Hopkins University, Baltimore; Dr. T. F. Robinson and Dr. E. L. Yellin, Department of Medicine, Albert Einstein College of Medicine, New York; Dr. G. Pelle, Laboratoire de Mécanique

Physique, University of Paris Val-de-Marne; and Dr. J. Tyberg, Departments of Medicine and Medical Physiology, University of Calgary.

Received for publication 14 December 1987 and in final form 27 May 1988.

REFERENCES

Bogen, D. K. 1987. Strain energy descriptions of biological swelling I: Single fluid compartment models. *ASME J. Biomech. Eng.* 109:252–256.

Borg, T. K., and J. B. Caulfield. 1979. Collagen in the heart. *Tex. Rep. Biol. Med.* 39:321–333.

Borg, T. K., and J. B. Caulfield. 1981. The collagen matrix of the heart. *Fed. Proc.* 40:2037–2041.

Borg, T. K., W. F. Ranson, F. A. Moslehy, and J. B. Caulfield. 1981. Structural basis of ventricular stiffness. *Lab. Invest.* 44:49–54.

Caulfield, J. B., and T. K. Borg. 1979. The collagen network of the heart. *Lab. Invest.* 40:364–372.

Chadwick, R. S. 1981. The myocardium as a fluid-fiber continuum: passive equilibrium configurations. *Adv. Bioeng.* 135–138.

Chadwick, R. S. 1982. Mechanics of the left ventricle. *Biophys. J.* 39:279–288.

Demer, L. L., and F. C. P. Yin. 1983. Passive biaxial mechanical properties of isolated canine myocardium. *J. Physiol. (Lond.).* 339:615–630.

Feit, T. S. 1979. Diastolic pressure–volume relation and distribution of pressure and fiber extension across the wall of a model left ventricle. *Biophys. J.* 28:143–166.

Fung, Y. C. 1984. Biodynamics: Circulation. Springer-Verlag, New York. 68–71.

Heineman, F. W., and J. Grayson. 1985. Transmural distribution of intramyocardial pressure measured by micropipette technique. *Am. J. Physiol.* 249 (*Heart Circ. Physiol.* 18):H1216–H1223.

Humphrey, J. D., and F. C. P. Yin. 1987. A new constitutive formulation for characterizing the mechanical behavior of soft tissues. *Biophys. J.* 52:563–570.

Lenkiewicz, J. E., M. J. Davies, and D. Rosen. 1972. Collagen in human myocardium as a function of age. *Cardiovasc. Res.* 6:549–555.

Ohayon, J., R. S. Chadwick, and C. Oddou. 1987. Effet d'une excitation intramyocardique radiale et uniforme sur la mécanique du ventricule gauche: étude théorique. *C. R. Acad. Sci. Paris Sér.* II. 305:335–338.

Ohayon, J., and R. S. Chadwick. 1988. Theoretical analysis of the effects of a radial activation wave and twisting motion on the mechanics of the left ventricle. *Biorheology.* 25:435–447.

Pelle, G., J. Ohayon, C. Oddou, and P. Brun. 1984. Theoretical models in mechanics of the left ventricle. *Biorheology.* 21:709–722.

Peskin, C. S. 1975. Mathematical Aspects of Heart Physiology. Courant Institute of Mathematical Sciences, New York.

Printzen, F. W., T. Arts, G. J. van Der Vusse, W. A. Coumans, and R. S. Reneman. 1986. Gradients in fiber shortening and metabolism across ischemic left ventricular wall. *Am. J. Physiol.* 250 (*Heart Circ. Physiol.* 19):H255–H264.

Robinson, T. F., L. Cohen-Gould, and S. M. Factor. 1983. Skeletal framework of mammalian heart muscle: arrangement of inter- and pericellular connective tissue structures. *Lab. Invest.* 49:482–498.

Robinson, T. F., S. M. Factor, and E. H. Sonnenblick. 1986. The heart as a suction pump. *Sci. Am.* (April) 254:84–91.

Robinson, T. F., S. M. Factor, J. M. Capasso, B. A. Wittenberg, O. O. Blumenfeld, and S. Seifter. 1987. Morphology, composition, and function of struts between cardiac myocytes of rat and hamster. *Cell Tissue Res.* 249:247–255.

Sagawa, K., 1978. The ventricular pressure-volume diagram revisited. *Circ. Res.* 43:677–687.

Sommerfeld, A. 1950. Mechanics of Deformable Bodies. Academic Press, Inc., New York.

Spencer, A. J. M. 1972. Deformations of Fibre-reinforced Materials. Clarendon Press, Oxford.

Streeter, D. D. 1979. Gross morphology and fiber geometry of the heart. *Handb. Physiol.* (Sect. 2):61–112.

ter Keurs, H. E. D. J., W. H. Rijusburger, R. van Heumingen, and M. J. Nagelsmit. 1980. Tension development and sarcomere length in rat cardiac trabeculae. *Circ. Res.* 46:703–714.

Tözeren, A. 1983. Static analysis of the left ventricle. *J. Biomech. Eng.* 105:35–46.

Tözeren, A. 1986. Assessment of fiber strength in a urinary bladder by using experimental pressure volume curves: an analytical method. *J. Biomech. Eng.* 108:301–305.

Tyberg, J. V., W. J. Kern, E. H. Sonnenblick, and C. W. Urschel. 1970. Mechanics of ventricular diastole. *Cardiovasc. Res.* 4:423–428.

Yellin, E. L., M. Hori, C. Yoran, E. H. Sonnenblick, S. Gabbay, and R. W. M. Frater. 1986. Left ventricular relaxation in the filling and nonfilling intact canine heart. *Am. J. Physiol.* 250 (*Heart Circ. Physiol.* 19):H620–629.